*AMSE JOURNALS-AMSE IIETA publication-2017-Series: Modelling A; Vol. 90; N°2; pp 181-192*
*Submitted Mar. 11, 2017; Revised May 10, 2017; Accepted Jun. 05, 2017*

# Analysis of the Fault Property of the Sensors in H-Bridge Converter

*Xiaodong Yang, **Wenyong Duan, ***Jiangang Wang, ****Guowen Hu

* School of Electrical Engineering, Yancheng Institute of Technology, Yancheng 224001, China (Corresponding author email: 24661883@qq.com)
** School of Electrical Engineering, Yancheng Institute of Technology, Yancheng 224001, China (dwy1985@126.com)
*** School of Electrical Engineering, Yancheng Institute of Technology, Yancheng 224001, China (wangjg@ycit.cn)
**** School of Electrical Engineering, Yancheng Institute of Technology, Yancheng 224001, China (hugw@ycit.cn)

## Abstract

Taking the various sensors in the H-bridge converter as the research object, this paper makes a characteristic analysis of their disconnection fault. First, the MATLAB simulation model for 8 cascaded H-bridge converters is established in the paper; then, the disconnection faults of the capacitance voltage sensor, system voltage sensor, load current sensor and output circuit sensor are simulated herein respectively; at last, the impact of disconnection fault of different sensors on the key parameters of the system is analyzed. The analysis results show that the disconnection faults of the system voltage sensor and the output circuit sensor have a relatively large impact on the system's key parameters. Therefore, certain measures must be taken to prevent the disconnection fault.

## Key words

H-bridge converter, Sensor fault, Fault property.

## 1. Introduction

With the wide application of power electronic technology in reactive compensation, harmonic control, DC transmission and so on, the reliability research such as the fault diagnosis and fault-

tolerant control of various power electronic systems has become the research focus of both domestic and foreign scholars currently.

The power electronic system is mainly composed of the switching devices, energy storage components, controllers and a variety of detection sensors. In order to ensure the reliable operation of the system, corresponding electrical protection (drive circuit, overcurrent protection, overvoltage protection, etc.) and thermal protection (heat dissipation structural design and overheating detection) are usually provided to the switching devices (such as IGBT, and freewheeling diode), energy storage components (DC-link capacitor, and filter inductance) and other key components. With the development of the power electronic technology, these conventional protections have become the standard configuration of these key components. In addition, in recent years domestic and foreign scholars have carried out in-depth research on the fault property of the switching devices [1-4] and the energy storage components [5-9], putting forward a variety of fault diagnosis methods and fault-tolerant control strategies [10-12].

The current fault diagnosis research in the power electronic field is mostly concentrated in the above aspects, and there are fewer researches on the fault of various test sensors.

The sensor is a key device in the power electronic system to detect various signals. Its reliability directly affects the normal operation of the system. With the continuous development of large-capacity converters, their internal operating environment is a strong electromagnetic environment with high frequency, high voltage, and heavy current, leading to more faults of the sensor which is installed inside the converter to test the voltage and current of its components.

In the closed-loop control process of the power electronic system, the feedback input is basically the signals detected by the sensor. If the sensor fails, it will cause the detection signal distortion or even make the signal disappear. If the fault is not handled in time, the feedback signals from the faulted sensor will quickly spread in the closed-loop control system, which may lead to the increase of the system's harmonic wave and equipment damage, even security incidents and casualties.

## 2. Simulation Model

By virtue of the tool of MATLAB/SIMULINK, a simulation model of the 10/6 KV medium-pressure cascade static synchronous compensator (STATCOM) is established in this paper, which serves as the research object. Its overall structure is as shown in figure 1.

Its main components include power supply system, LCL filter, soft start, converter, load, etc. In the diagram, $i_s$ refers to the system's current, $i_l$ stands for the current of the load machine, $i_c$

means the device's current (behind the LCL filter), $i_{cl}$ also means the device's current (in front of the LCL filter), and $i_f$ represents the current of the LCL filter capacitor.

Each phase of the converter is composed of 8 H-bridge power modules in series. A neutral common point is formed in one side in the form of star between the three phases and the other end is connected to the power supply system via LCL filter.

The control strategy of the simulation model is the decoupling control based on abc/dq conversion. The overall structure of the control is as shown in Figure 2. The calculation of the command current is as shown in Figure 3. The command current is divided into active current command and reactive current command. $\sum U_{dc}$ is the sum of the actual detection values of the DC-side capacitor voltage of each H-bridge unit. It can be seen from the figure that the changes of the value of the DC-side current and voltage, the system voltage value and the load current value directly affect the command current. So if these sensors fail, they will make the command current change, thus affecting the system's output voltage, output current and harmonic content.

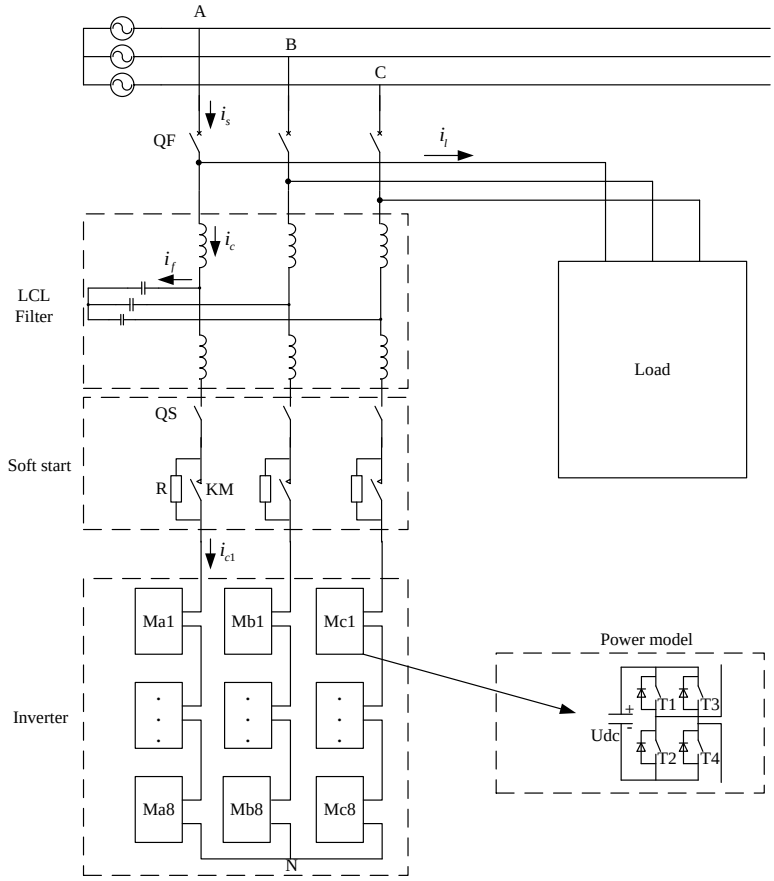


Fig.1. Overall Structural Diagram of the Simulation Model

In addition, in the decoupling control, after the system's output current goes through the conversion of abc/dq coordinates, the actual current in the dq coordinate system is obtained, and

then the regulation control is made after making a comparison analysis of the actual current and the command current in the dq coordinate system. Therefore, whether the system's output current sensor operates normally or not also directly affects the system's operation.

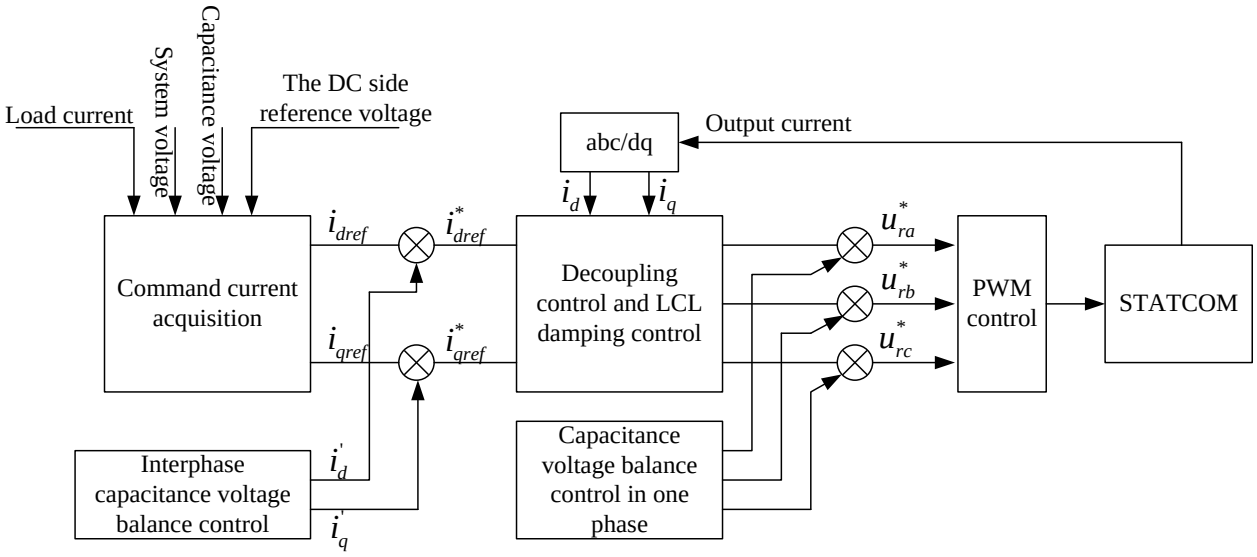


Fig.2. Overall structure of the control system

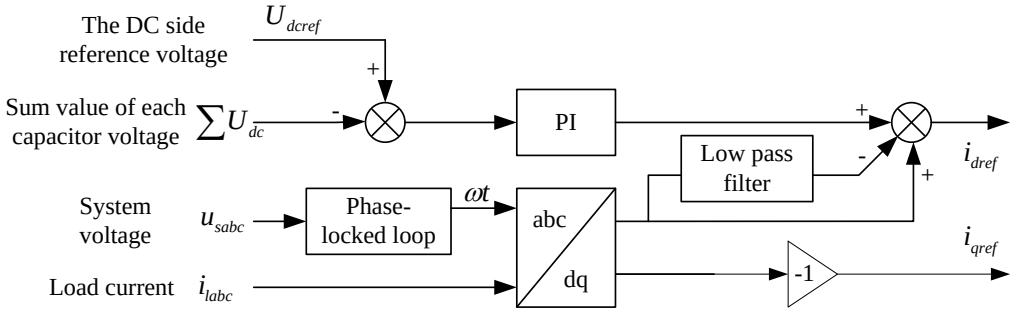


Fig.3. The calculation of the command current

## 3. Classification of the Sensor Faults

Common faults of the sensor include stuck fault, constant gain variation and constant deviation failure, which are generally caused by the aging, precision degradation and drifting of the components and parts during the usage of the sensor. The value of amplitude of these types of faults is generally small, thus they are not easy to be found.

The simulation of the stuck failure, constant gain variation and constant deviation failure can be carried out using the fault simulation method shown in Table 1.

Here, u(i) and $\tilde{u}(i)$ represent the actual output of the sensor under the fault condition and normal condition respectively. A and $\Delta\varepsilon$ are constants and $\beta$ is a proportionality coefficient.

Among them, the disconnection fault is the most common one in the stuck fault (The constant value of the sensor output A=0). Taking the disconnection of the capacitance voltage sensor with the Mal power; module and Phase A current as an example, and the simulation of its fault is as shown in Figure 1.

Tab.1. Sensor Fault Type and Simulation

| Failure Description | | |
|---|---|---|
| Fault Type | Mathematical Expression | Fault Simulation Method |
| Stuck | $u(i)=A$ | Impose the constant step signals to the sensor output |
| Constant gain | $u(i)=\beta\tilde{u}(i)$ | Impose constant ramp signals to the original signals |
| Constant deviation | $u(i)=\tilde{u}(i)+\Delta\varepsilon$ | Impose the constant step signals to the original signals |

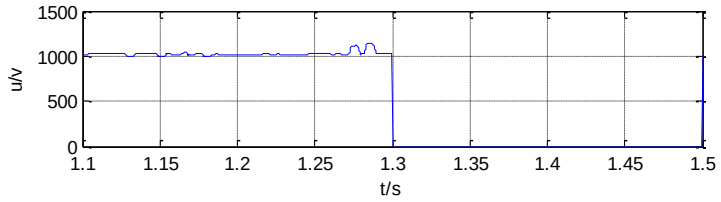


Fig.4. Capacitance Voltage Sensor Fault Simulation of Phase A

## 4. Faults Analysis of the Fault of Capacitance Voltage Sensor

Figure 5 presents the simulation waveforms of the system current is, the load current il, the output current ic, the command current id at the d axis and the command current iq at the q axis under the normal condition of the capacitance voltage sensor and when there is a disconnection fault (at the place of 1.3s in the figure) of the Phase-A capacitance voltage sensor of Mal power module. It can be seen from the figure that the waveform of each parameter does not change obviously before and after the fault.

Figure 6 shows the simulation waveform of the sum of the Phase-A capacitance voltages before and after the fault. It can be seen from the figure that after the fault, there is an obvious fluctuation in the waveform, which comes closer to balance soon later.

Figure 7 presents the simulation waveforms of the three-phase capacitance voltages of each power module. It can be seen from the figure that there is no obvious abnormality in Phase-B and Phase-C capacitance voltages of different power modules. For Phase-A, the capacitance voltage of other modules all rises steadily, except that the capacitance voltage of Mal module changes to 0.

It is the functions of the internal balance control strategy and the interphase balance control strategy. When the capacitance voltage of certain module is abnormal, the voltage values of other

modules could be adjusted rapidly to realize balance control, thus making the sum of the Phase-A capacitance voltage remain within a stable range.

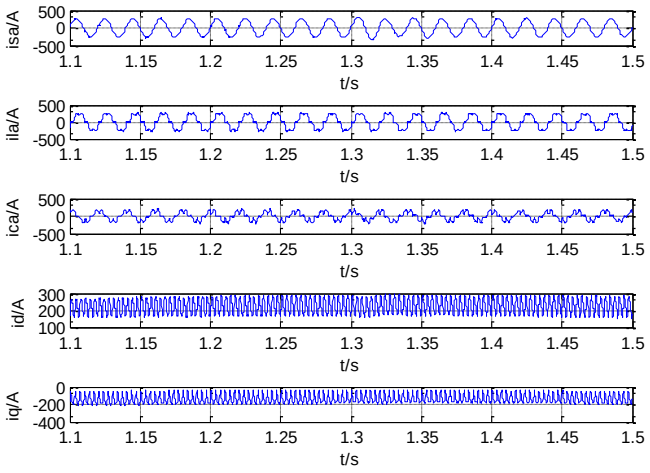


Fig.5. System Current, Load Current, Compensating Current and dq Axis Command Current

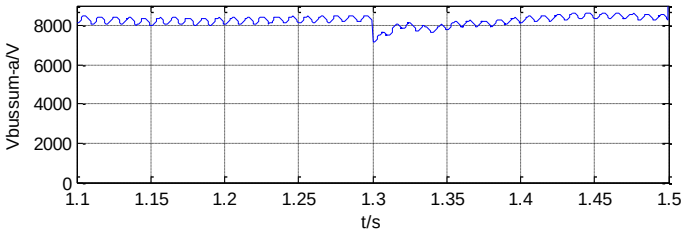


Fig.6. Sum of the Phase-A Capacitance Voltage Current Before and After the Fault

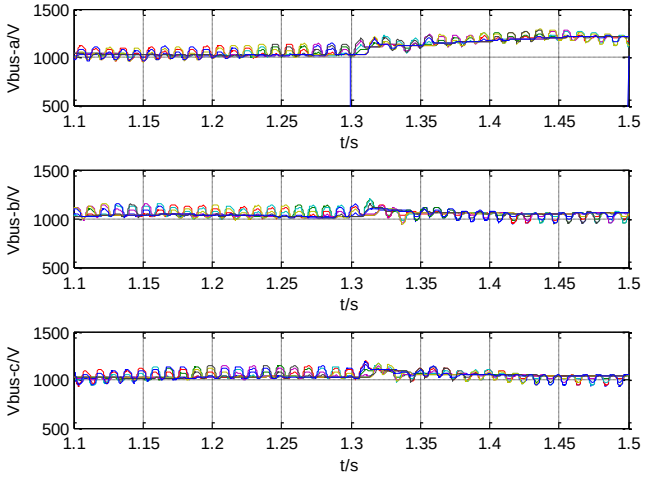


Fig.7. The Capacitance Voltage of each Module Before and After the Fault

## 5. Analysis of the Fault of the System Voltage Sensor

Figure 8 presents the simulation waveforms of the system current isa, the load current ila, the

output current ica, the command current id at the d axis and the command current iq at the q axis under the normal condition of the system voltage sensor and when there is a disconnection fault (at the place of 1.3s in the figure) of the Phase-A system voltage sensor. It can be seen from the figure that the waveform of each parameter does not change obviously before and after the fault.

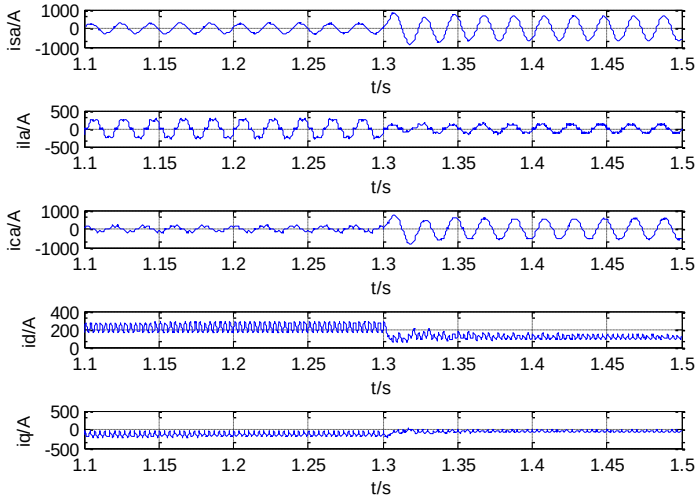


Fig.8. Waveforms of the System Voltage Sensor Before and After the Disconnection Fault

Figure 9-11 indicates the change of the actual value of the Phase-A, Phase-B and Phase-C capacitance voltage of each power module before and after the sensor fault

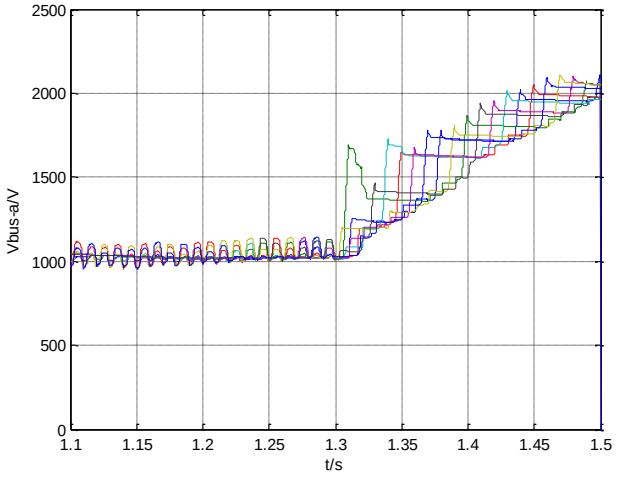


Fig.9. Phase-A Capacitance Voltage of Each Module Before and After the Disconnection Fault of the System Voltage Sensor

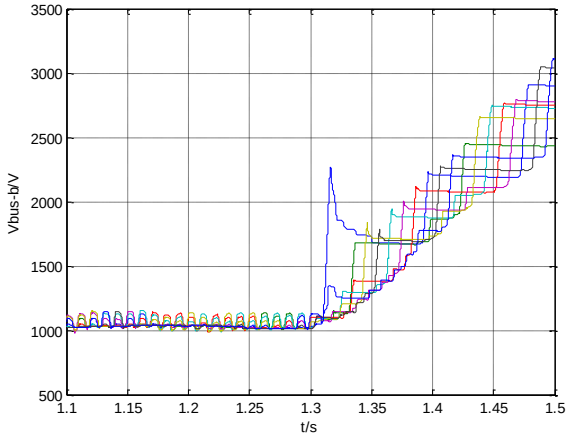


Fig.10. Phase-B Capacitance Voltage of Each Module Before and After the Disconnection Fault of the System Voltage Sensor

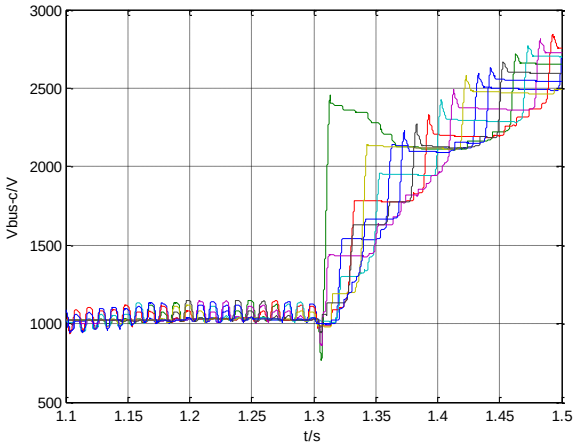


Fig.11. Phase-C Capacitance Voltage of Each Module Before and After the Disconnection Fault of the System Voltage Sensor

It can be seen from the figure that when the fault occurs, there is relatively large fluctuation in the capacitance voltage of each power module and the interphase capacitance voltage is no longer balanced, which may affect the system's output side, or even cause the capacitance trouble. Under this circumstance, if the system is overcharged, the capacitance may explode. Therefore, it is necessary to detect the fault of the system voltage sensor of each power module and carry out the fault-tolerant control.

## 6. Analysis of the Fault of the Load Current Sensor

Figure 12 presents the simulation waveforms of the system current isa, the load current ila, the output current ica, the command current id at the d axis and the command current iq at the q axis

under the normal condition of the load current sensor and when there is a disconnection fault (at the place of 1.3s in the figure) of the Phase-A load current sensor. It can be seen from the figure that the waveform of each parameter, except for the load current, does not change obviously before and after the fault.

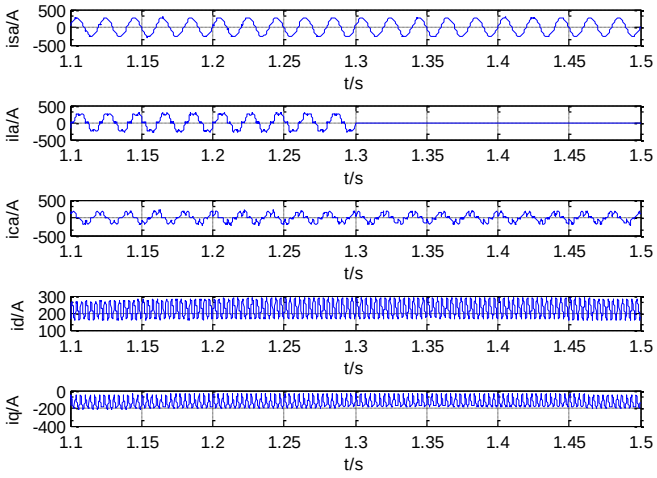


Fig.12. The Waveforms of the Load Current Sensor Before and After the Disconnection Fault

Figure 13 shows the change of the actual value of Phase-A, Phase-B and Phase-C capacitance voltage of each power module before and after the sensor fault. It can be seen from the figure that after the fault, there is an obvious fluctuation in the waveform, which comes closer to balance soon later.

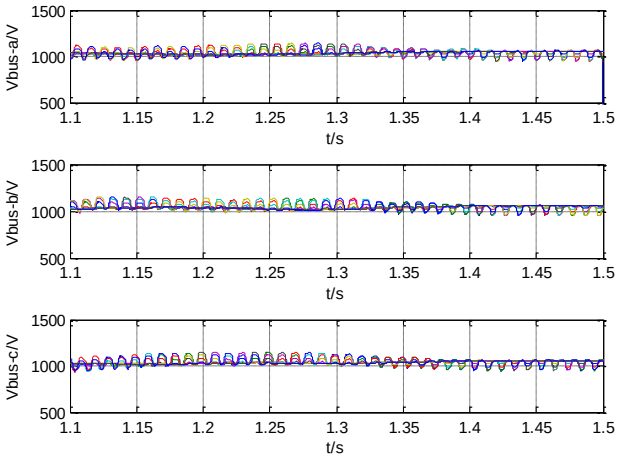


Fig.13. The Three-phase Capacitance Voltage of Each Module of the Load Current Sensor Before and After the Disconnection Fault

## 7. Analysis of the Fault of the Output Current Sensor

Figure 14 presents the simulation waveforms of the system current isa, the load current ila, the output current ica, the command current id at the d axis and the command current iq at the q axis under the normal condition of the load current sensor and when there is a disconnection fault (at the place of 1.3s in the figure) of the Phase-A output current sensor. It can be seen from the figure that the waveform of each parameter changes dramatically in terms of amplitude and harmonic wave before and after the fault.

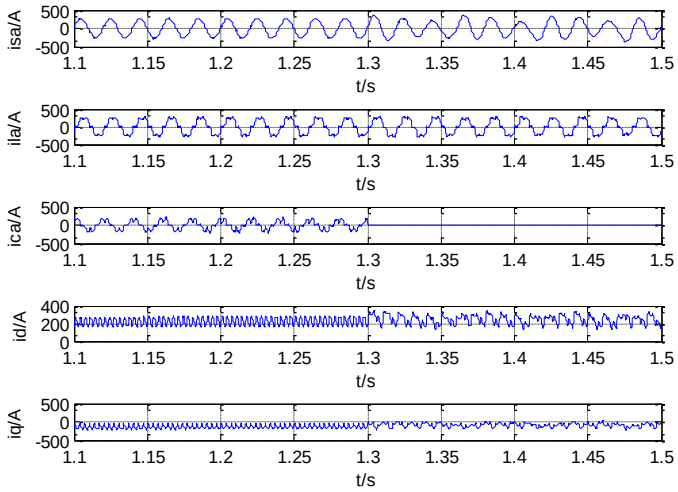


Fig.14. Waveform of the Output Current Sensor Before and After the Disconnection Fault

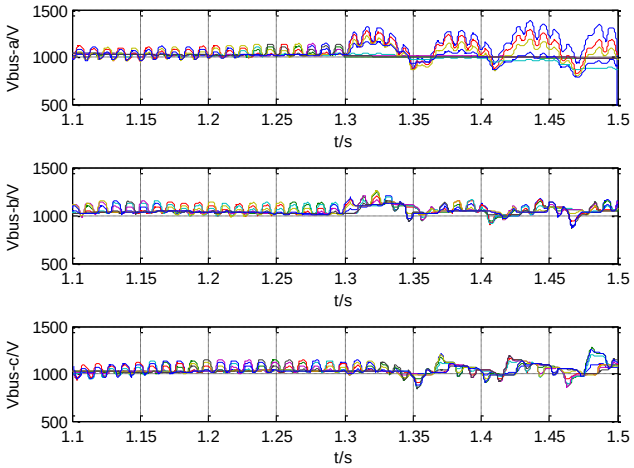


Fig.15. The Three-phase Capacitance Voltage of Each Module of The Output Current Sensor Before and After the Disconnection Fault

Figure 15 shows the change of the actual value of Phase-A, Phase-B and Phase-C capacitance voltage of each power module before and after the sensor fault. It can be seen from the figure that

after the fault, there is an obvious fluctuation in the amplitude of the capacitance voltage of each module, especially of the Phase-A capacitance voltage of each module.

## Conclusion

Taking the 8 cascaded STATCOM simulation model with H-bridge structure as the research object, this paper makes a simulation analysis of the disconnection fault of various kinds of sensors and the following conclusions are drawn:

(1) The disconnection fault of the system voltage sensor and output current sensor have a large impact on the system' s parameters, causing apparent change in the system output amplitude, harmonic wave, etc. In addition, the disconnection fault also exerts large impact on the charging and discharging of the capacitance voltage of each module. The capacitance damage or even explosion may occur in the actual device. Therefore, it is a must to carry out fault diagnosis and fault-tolerant control over the faults of these two kinds of sensors.

(2) After the occurrence of the disconnection fault of the capacitance voltage sensor and the load current sensor, there will be a temporary wave in the parameters of the system, but they will tend to be stable soon. Therefore, for these two kinds of faults, the fault diagnosis and alarm could be adopted.

The following further researches will be carried out:

(1) Establishing fault mathematic model to infer the parameter variation mechanism in a theoretical way and form an inner relationship between different faults and parameter variation.

(2) Select suitable original signal based on the simulation and computation result, and extract the fault features, thus providing basis for the fault diagnosis.

## References


1. X. Sun, X. Tong, X. Gao, Research on the fault diagnosis of IGBT valve in VSC-HVDC, 2014, Transactions of China Electrotechnical Society, vol. 29, no. 8, pp. 235-241, 264.
2. L.M.A. Caseiro, A.M.S. Mendes, Real-Time IGBT Open-Circuit Fault Diagnosis in Three-Level Neutral-Point-Clamped Voltage-Source Rectifiers Based on Instant Voltage Error, 2015, Industrial Electronics IEEE Transactions on, vol. 62, no. 3, pp. 1669-1678.
3. M.A. Rodríguez-Blanco, A. Vázquez-Pérez, L. Hernández-González, et al., Fault Detection for IGBT Using Adaptive Thresholds During the Turn-on Transient, 2015, IEEE Transactions on Industrial Electronics, vol. 62, no. 3, pp. 1975-1983.
4. P. Sai Prasanna, M. Sreedhar, L.V.S. Kumar, A review on circulating current suppression control, capacitor voltage balancing and fault analysis of modular multilevel converters, 2015,

International Conference on Electrical, Electronics, Signals, Communication and Optimization. IEEE, pp. 1-6.

5. H. Mobki, M.H. Sadeghi, G. Rezazadeh, Design of Direct Exponential Observers for Fault Detection of Nonlinear MEMS Tunable Capacitor, 2015, International Journal of Engineering, - Transactions, A: Basics, vol. 28, no. 4, pp. 634-641.
6. J. Druant, T.J. Vyncke, J.A. Melkebeek, Adding inverter fault detection to model-based predictive control for flying-capacitor inverters, 2013, IEEE International Symposium on Sensorless Control for Electrical Drives and Predictive Control of Electrical Drives and Power Electronics. IEEE, pp. 1-5.
7. A.A. Elserougi, A.M. Massoud, S. Ahmed, A Switched-Capacitor Submodule for Modular Multilevel HVDC Converters With DC-Fault Blocking Capability and a Reduced Number of Sensors, 2016, IEEE Transactions on Power Delivery, vol. 31, no. 1, pp. 313-322.
8. F. Ezzahra, M. Hamouda, J. Ben, Real-Time implementation of an Open-Circuit Dc-Bus Capacitor Fault diagnosis method for a Three-Level NPC Rectifier, 2016, International Journal of Advanced Computer Science & Applications, vol. 7, no. 11, pp. 243-247.
9. H. Givi, E. Farjah, T. Ghanbari, Switch fault diagnosis and capacitor lifetime monitoring technique for DC–DC converters using a single sensor, 2016, Iet Science Measurement & Technology, vol. 10, no. 5, pp. 513-527.
10. T. Li, C. Zhao, Characteristic analysis and fault-tolerant control of modular multilevel converters under sub-module faults, 2016, International Transactions on Electrical Energy Systems, vol. 26, no. 7, pp. 1444-1461.
11. M. Gleissner, M.M. Bakran, Design and Control of Fault-Tolerant Nonisolated Multiphase Multilevel DC–DC Converters for Automotive Power Systems, 2016, IEEE Transactions on Industry Applications, vol. 52, no. 2, pp. 1785-1795.
12. I. Gonzalez-Prieto, M.J. Duran, F.J. Barrero, Fault-tolerant Control of Six-phase Induction Motor Drives with Variable Current Injection, 2016, IEEE Transactions on Power Electronics, vol. 32, no. 10, pp. 7894-7903.